Accurately calculating the collision probability using a Gaussian mixture method to propagate orbital uncertainty

Ruidong Yan[1], Jiancun Gong, Siqing Liu, Ronglan Wang, Liqin Shi
National Space Science Center, Chinese Academy of Science, Beijing, 100190, China;
School of Chinese Academy of Science, Beijing, 100190, China;

1. Introduction

Currently, more than 19,000 pieces of debris with a diameter exceeding 10 cm have been catalogued around the Earth. Consequently, collision warning systems are of great significance, especially for low Earth orbit (LEO) space assets. For an encounter between two objects, the US Joint Space Operations Center (JSpOC) can compute and report a value commonly referred to as a collision probability, which can be used by a satellite owner/operator as a warning and may motivate a personal investigation of the collision. Other countries, including China, have also established collision warning programmes to protect their spacecrafts. The collision probability is an accepted and calibrated parameter for evaluating the collision between two space objects. (Foster and Estes 1992), (Patera 2001&2005), (Chan 1997&2004&2003), and (Alfano 2005) have developed methods for calculating the collision probability. Foster derived the collision probability by applying polar coordinates in the encounter plane, which is perpendicular to the relative velocity of the two objects; hence, in this approach, the probability density function (PDF) is expressed as a polar parameter. This collision probability model is currently applied by NASA to assess the on-orbit collision risk for the International Space Station. Chan used series expansion to analytically approximate the collision PDF; in this technique, the three-dimensional Gaussian probability density function is transformed into a two-dimensional PDF by projecting the Gaussian covariance onto the encounter plane. This model is currently applied in the Analytical Graphics, Inc., Satellite Tool Kit. A mathematically equivalent expression was developed by Patera to represent the collision PDF, and this method is implemented within the Collision Vision Tool by the Aerospace Corporation. Alfano's method employs series expansion to represent the collision PDF. (Alfano 2009) applied a simplified Monte Carlo process based on a two-body analytical propagation to assess the satellite collision probability computations with different methods. Alfano provided 12 test cases involving linear and nonlinear relative motion for satellites in geosynchronous orbit (GEO) and LEO, as well as nonlinear relative motion for highly eccentric orbit (HEO), and compared the accuracy of each method with that of the Monte Carlo method. In addition to the methods mentioned above, many scholars have employed the Monte Carlo method to calculate the collision probability. (Sabol, Binz et al. 2011) used a special perturbation-based Monte Carlo method to investigate approaches for estimating the probability of collision between two satellites. Comparisons were made against an analytical method and a two-body Monte Carlo method for LEO and GEO satellites. (de Vries and Phillion 2010) calculated the collision

[1] Corresponding author
Email address: yanruidong@nssc.ac.cn (Ruidong Yan)

probability using a Monte Carlo approach that requires knowledge of the full 6x6 covariance matrix information for each of the objects and is capable of incorporating not only the positional uncertainty but also the velocity uncertainty. (Morselli, Armellin et al. 2015) developed a differential algebra (DA)-based Monte Carlo simulation that was introduced to further improve the efficiency and accuracy of the Monte Carlo collision probability computation. As shown above, the Monte Carlo method is the most accurate approach for calculating short-term or long-term encounter collision probabilities; however, this technique is computationally intensive.

In this paper, a new Gaussian mixture method combined with a linear and UT covariance method is used to propagate the orbital uncertainty. Then, Chan's method is applied to calculate the collision probability between two objects according to the relative position and orbital uncertainty. The remainder of this paper is organized as follows. The orbit perturbation dynamics model and orbital error are briefly reviewed in Section 2. Section 3 describes the results of numerical experiments, and the conclusions are provided in Section 4.

2. Methodology

2.1 Determination of the Gaussian mixture components

Determining the Gaussian mixture component covariance is the key step in approximating the initial orbital covariance distribution. (Psiaki, Schoenberg et al. 2015) introduced a Gaussian mixture component covariance determination algorithm. Referring to this algorithm, the square root information matrix is set as

$$P_j = R_j^{-1} R_j^{-T}, j = 1, \cdots, N \tag{1}$$

To guarantee the error propagation accuracy of the linear and UT methods, an upper bound is set for the component covariance matrix of the Gaussian mixture. This means that there is a lower bound for $R_j^T R_j, (j = 1, \cdots, N)$:

$$R_j^T R_j \geq R_{\min}^T R_{\min}, j = 1, \cdots, N \tag{2}$$

Both sides of this inequality are symmetric matrices, and the inequality indicates that the left side minus the right side creates a positive semi-definite matrix.

$$P_j = R_j^{-1} R_j^{-T} \leq R_{\min}^{-1} R_{\min}^{-T} = P_{\max}, j = 1, \cdots, N \tag{3}$$

The selection of $P_{\max}$ needs to take into account all the nonlinearity of the measurement model and dynamical system. A linear Taylor series approximation of the nonlinearities over the range of state perturbations Δx is required to satisfy the bounds as follows:

$$\Delta x^T P_{\max}^{-1} \Delta x \leq \rho, 1 \leq \rho \leq 3 \tag{4}$$

At the same time, the covariance matrix of the Gaussian mixture components must be less than the initial orbit covariance matrix. If the square root information matrix of the initial orbit covariance is assumed to be R_0, then the Gaussian component square root information matrix is satisfied:

$$R_j^T R_j \geq R_0^T R_0,\ j = 1,\cdots,N \tag{5}$$

In addition to satisfying inequality (13), to prevent the component covariance matrix from being too small while using an appropriate number of component covariances to fit the orbit covariance, the traces of the matrices $R_0^{-T} R_j^T R_j R_0^{-1}$ and $R_{\min}^{-T} R_j^T R_j R_{\min}^{-1}$ should be minimized. To calculate the optimal solution of a linear matrix inequality, first, singular value decomposition is applied to the matrix $R_0 R_{\min}^{-1}$:

$$U_j S_j V_j^T = R_0 R_{\min}^{-1} \tag{6}$$

where U_j and V_j are orthogonal matrices and S_j is a diagonal matrix whose diagonal line is a singular value $\sigma_{j1},\cdots\sigma_{jn}$. If $k = 1,\cdots,n\ \sigma_{jk} \geq 1$, then $R_j = R_0$ is the optimal solution satisfying the linear matrix inequalities of equations (10) and (13). Otherwise, the following diagonal matrix is given:

$$\delta S_{jfull} = \begin{bmatrix} \sqrt{\max(1-\sigma_{j1}^2, 0)} & \cdots & 0 \\ \vdots & \ddots & \vdots \\ 0 & \cdots & \sqrt{\max(1-\sigma_{jn}^2, 0)} \end{bmatrix} \tag{7}$$

Then, the row in δS_{jfull} for which all the values are zero is deleted to form the matrix δS_j, that is, row k in δS_{jfull} is deleted for every k such that $\sigma_{jk} \geq 1$. The resulting matrix is then used to generate the following matrix:

$$\delta R_j = \delta S_j V_j^T R_{\min} \tag{8}$$

Finally, orthogonal/upper-triangular (QR) matrix decomposition is used to calculate R_j, the formula for which is as follows:

$$Q_j \begin{bmatrix} R_j \\ 0 \end{bmatrix} = \begin{bmatrix} \delta R_j \\ R_0 \end{bmatrix} \tag{9}$$

where Q_j and R_j are an orthonormal matrix and a square, upper-triangular matrix, respectively. One can prove that matrix R_j satisfies inequalities (10) and (13). These properties indicate that $R_j^T R_j$ is as close as possible (in a matrix sense) to $R_{\min}^T R_{\min}$ and $R_0^T R_0$. Therefore, under the same probability density approximation, the number of Gaussian mixture components is reduced. The reduction of each Gaussian covariance relative to the initial covariance is

$$\delta P_j = P_0 - P_j = R_0^{-1} R_0^T - R_j^{-1} R_j^{-T} = \delta Y_j \delta Y_j^T \tag{10}$$

This covariance decrement is positive semi-definite, and δY_j, which is its matrix square root, can be computed using the following formula:

$$\delta Y_j = R_0^{-1} R_0^{-T} \delta R_j^T R_{dj}^{-1} \tag{11}$$

where R_{dj} is determined from QR matrix decomposition:

$$Q_{dj} \begin{bmatrix} R_{dj} \\ 0 \end{bmatrix} = \begin{bmatrix} R_0^{-T} \delta R_j^T \\ I \end{bmatrix} \tag{12}$$

where Q_{dj} is an orthonormal matrix and R_{dj} is a square, upper-triangular matrix.

The following steps outline the Gaussian mixture covariance calculation procedure.

1). The number of Gaussian mixture components is set as N. The number of columns in the covariance decrement square root matrix δY_j is $n_{\delta Y}$.

2). The current Gaussian component is set to be the *j*th Gaussian mixture term.

3). Then, an $n_{\delta Y}$-dimensional independent column vector $\boldsymbol{\eta}_j$ that follows a standard normal distribution is generated.

4). Singular value decomposition is applied to the matrix $R_0 R_{\min}^{-1}$ as $U_j S_j V_j^T = R_0 R_{\min}^{-1}$.

5). If $\sigma_{jk} \geq 1$ $k = 1, \cdots, n$, then $R_j = R_0$ is the optimal solution; otherwise, $\delta R_j = \delta S_j V_j^T R_{\min}$.

6). QR matrix decomposition is used to calculate R_j.

7). The mean of the *j*th Gaussian component is $\boldsymbol{\mu}_j = \boldsymbol{\mu}_0 + \delta \mathbf{Y}_j \boldsymbol{\eta}_j$.

8). The weight of the *j*th Gaussian component is $w_j = 1/N$.

9). Repeat step 2 until *j*=N.

The proper selection of $P_{\max}$ (or, equivalently, $R_{\min}$) that is suited for a particular application is critical to the implementation of this method. $R_{\min}$ shall be selected according to the size of the initial orbital covariance and the length of the orbital prediction time. For the simulation in Section 4, $R_{\min}$ is selected between $10R_0$ and $100R_0$. The larger the initial covariance or the longer the prediction time is, the greater the value of $R_{\min}$ will be; in contrast, the smaller the initial orbital covariance or the shorter the prediction time is, the smaller the value of $R_{\min}$ will be. In this paper, $R_{\min}=10R_0$ can meet the accuracy requirement of initial orbital uncertainty Gaussian mixing and propagation.

3. Simulation result

The uncertainty propagation methods employed above are further tested to compute the collision probability of two objects with a larger initial orbital uncertainty than that of the objects in simulation case 1. In this case, the initial orbital states of the two objects are the same as those in the first case; however, the initial uncertainty is greater than the uncertainty. The orbital states and covariance are propagated forward for 2 days, and 500 and 5,000 Gaussian mixture components are used in the simulation to approximate the initial orbital covariance. To compare the difference between the univariate splitting Gaussian mixture method and the proposed Gaussian mixture method, we also calculate the simulation results of the univariate splitting Gaussian mixture method. Because the eigenvalues of the orbital uncertainty covariance matrix play an important role in the selection of the splitting direction, the maximum eigenvector direction is selected as the splitting direction for the univariate splitting Gaussian mixture method. In addition, we choose 25 Gaussian mixture components from Vittaldev's univariate splitting library, and each Gaussian component is propagated by the UKF method. Thus, we compute the propagation of 325 points. Figure 1 plots the three-dimensional spatial distributions of the first object's orbital positional uncertainty predicted by the Monte Carlo method and the Gaussian mixture method for two days. The propagated positional uncertainty and the 3σ ellipsoids predicted by the Monte Carlo evolution method, Gaussian mixture method, linear method, UKF method and univariate splitting Gaussian mixture method are projected onto two coordinate planes, namely, the radial-intrack plane, radial-crosstrack plane and intrack-crosstrack plane, in figures 2, 3 and 4, respectively. Figures 1-4 show that after two days of propagating the initial orbital uncertainty, the distribution of Monte Carlo sampling points is no longer subject to a Gaussian distribution but instead displays a crescent-like shape in the radial direction. The linear method and UKF method still assume that the orbital distribution is Gaussian; the latter can describe the overall distribution of the orbital state but cannot provide the specific shape of the distribution, while the former cannot even represent the distribution of the orbital state. This is because the first two moments that correspond to the 3σ ellipsoids are insufficient to match the non-Gaussian distribution. Therefore, the linear method and the UKF method can no longer capture the characteristics of the non-Gaussian orbital uncertainty distribution. The Gaussian mixture method and the linear method are combined to decompose the initial covariance propagation into forecasts for multiple small Gaussian components. Consistent with the univariate splitting Gaussian mixture method, the Gaussian mixture method proposed herein is still effective at capturing the non-Gaussian distribution. Hence, the Gaussian mixture method can still be used to predict the orbital state distribution if the orbital distribution is non-Gaussian and can accurately represent the propagation characteristics of the orbital uncertainty under a large initial orbit covariance.

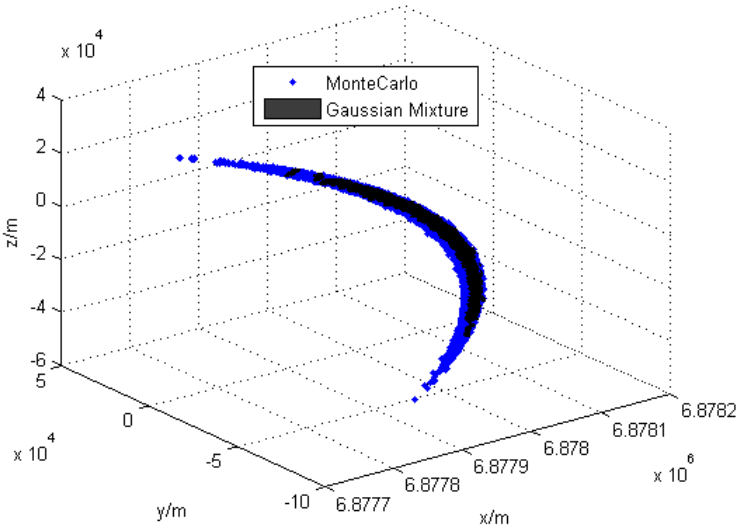

Figure 1 Distributions of the positional uncertainty results propagated by the Monte Carlo simulation and Gaussian mixture ellipsoid in three-dimensional space

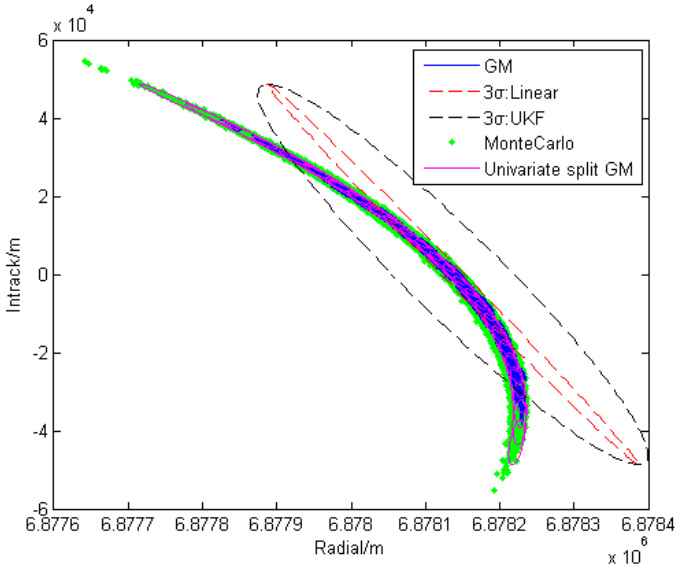

Figure 2 Radial-intrack plane projection of the positional uncertainty propagated by the Monte Carlo samples, Gaussian mixture ellipsoid, linear method, UKF method and Univariate splitting Gaussian mixture method

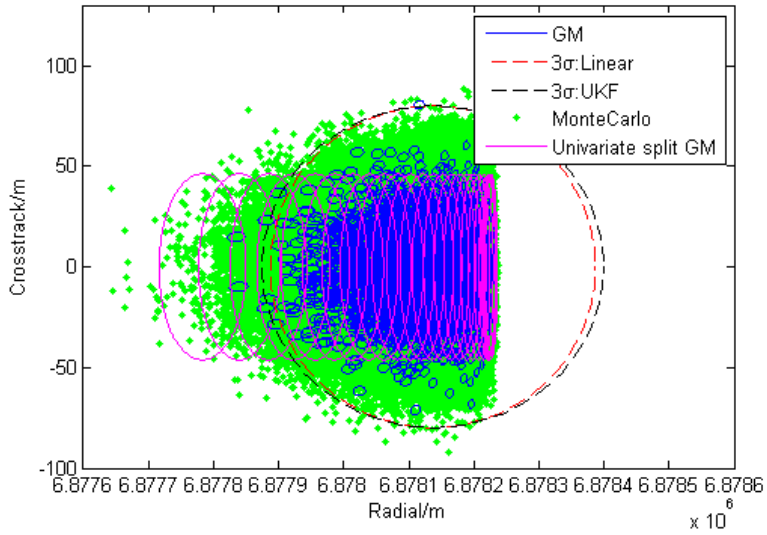

Figure 3 Radial-crosstrack plane projection of the positional uncertainty propagated by the Monte Carlo samples, Gaussian mixture ellipsoid, linear method, UKF method and Univariate splitting Gaussian mixture method

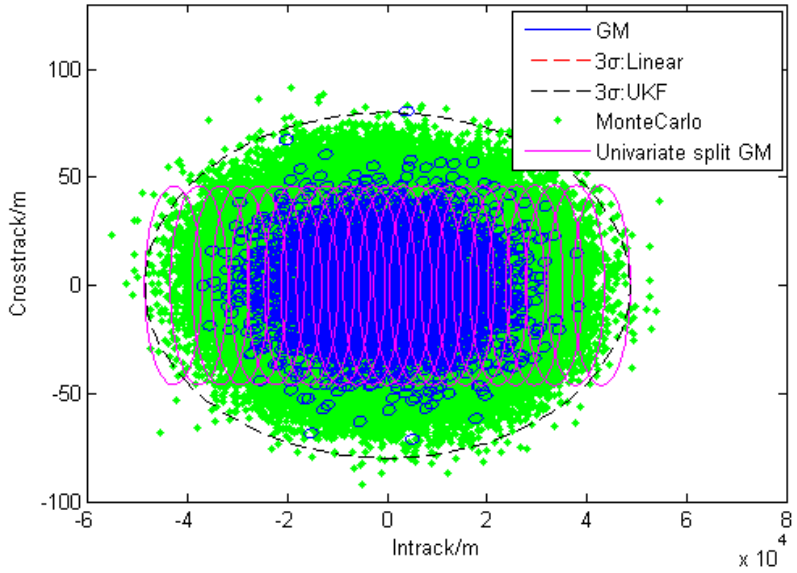

Figure 4 Intrack-crosstrack plane projection of the positional uncertainty propagated by the Monte Carlo samples, Gaussian mixture ellipsoid, linear method, UKF method and Univariate splitting Gaussian mixture method

Figures 15-17 show the probability density distributions of the first object's orbital error in the inertial coordinate system after propagation for 2 days by using 5 different methods. GM-500 and GM-5000 represent the probability density distributions using 500 and 5000 weighted Gaussian mixture components, respectively. The propagation results of the Monte Carlo samples are compared with those of the other methods. Figures 5-7 reveal that due to the influence of nonlinear terms, the prediction results of the linear method contain a large error, especially reflected in the direction of the

inertial x-axis, while the errors in the other directions are small. The prediction results of the Gaussian mixture method are basically consistent with those of the Monte Carlo simulation, especially in the direction of the inertial x-axis with a large linear error. Some fluctuations in the Gaussian mixture prediction results are observed, but increasing the number of Gaussian mixture components can effectively reduce the fluctuation amplitude. Although the prediction results have a certain random error, this error can be effectively suppressed by increasing the number of Gaussian mixture components to ensure that the prediction results approximate the exact solution. Compared with the univariate splitting method, the advantage of the proposed Gaussian mixture method is that it does not need to search for the most nonlinear direction. Moreover, the accuracy of the orbital uncertainty represented by the proposed Gaussian mixture method is correlated with the number of Gaussian mixture components: the more Gaussian mixture components there are, the higher the accuracy of the uncertainty representation will be.

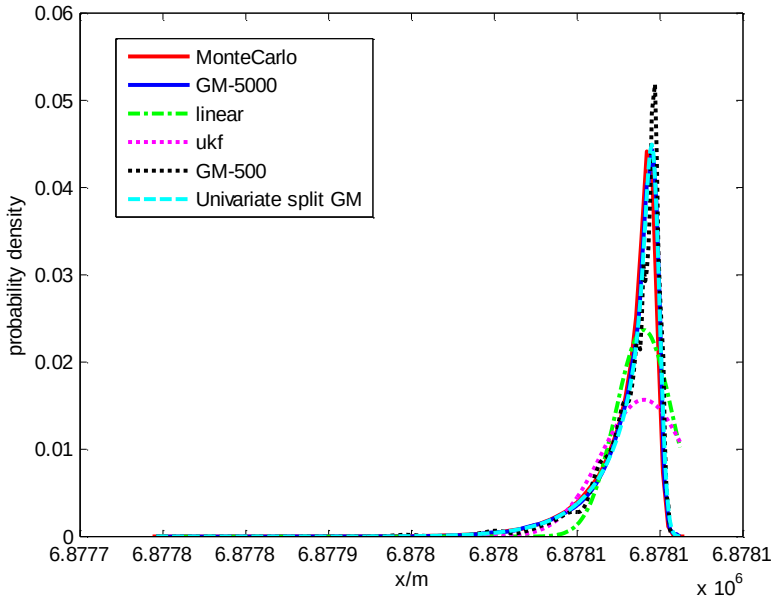

Figure 5 Probability density distributions of the positional uncertainty along the x-axis propagated by the Monte Carlo samples, Gaussian mixture ellipsoid, linear method, UKF method and Univariate splitting Gaussian mixture method

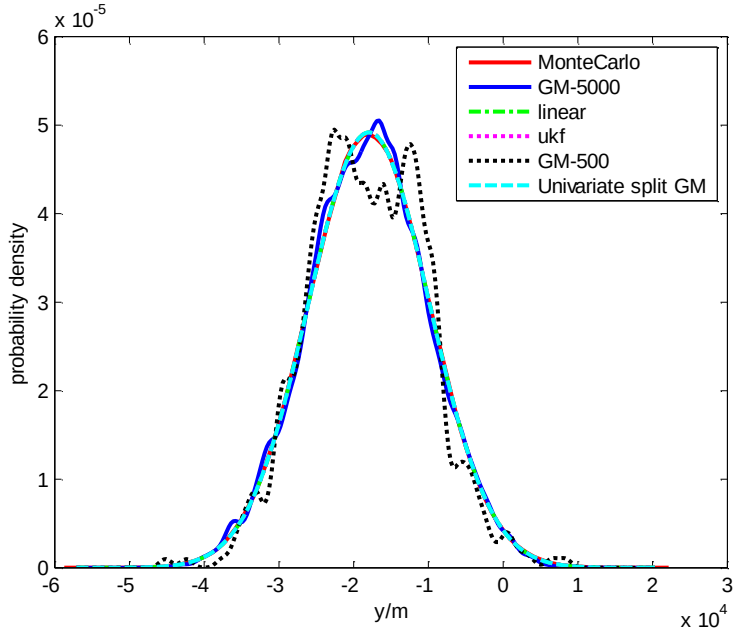

Figure 6 Probability density distributions of the positional uncertainty along the y-axis propagated by the Monte Carlo samples, Gaussian mixture ellipsoid, linear method, UKF method and Univariate splitting Gaussian mixture method

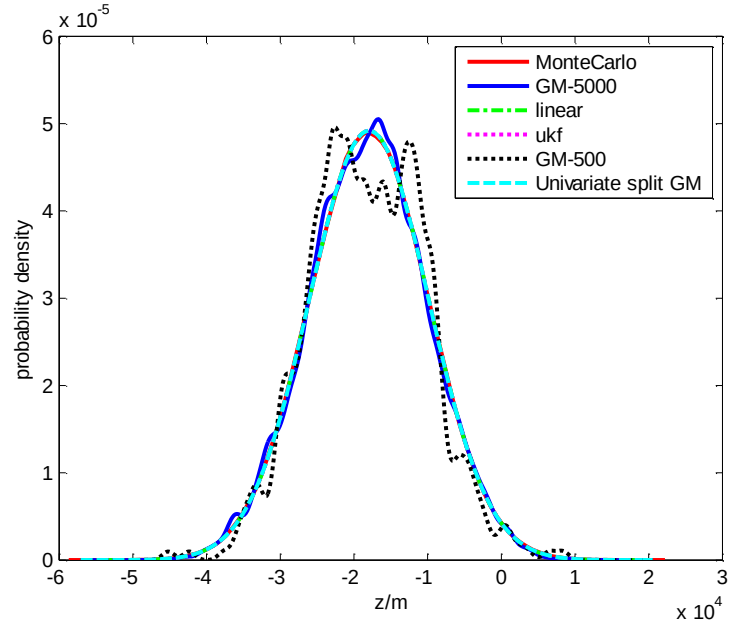

Figure 7 Probability density distributions of the positional uncertainty along the z-axis propagated by the Monte Carlo samples and Gaussian mixture ellipsoid, linear method, UKF method and Univariate splitting Gaussian mixture method

The method for propagating the orbital uncertainty for the second object is similar to that for the first object. The collision probability of the two objects is calculated according to the orbital state and error distribution propagated by the methods mentioned above. The collision probabilities of the two

objects calculated by the different methods are shown in table 2.

Table 1Collision probabilities computed using different uncertainty propagation methods

Method	Linear	UKF	GM-500	GM-5000	Univariate GM	Monte Carlo
Collision probability	6.784×10^{-4}	6.492×10^{-4}	1.2×10^{-3}	1.661×10^{-3}	1.46×10^{-3}	1.663×10^{-3}

Table 1 shows that the collision probabilities calculated by the linear method and UKF method are less than that calculated by the Monte Carlo method, and thus, their calculation accuracy cannot be used as the standard to predict the collision of space objects. In contrast, the collision probability calculated by the Gaussian mixture method is equal to that calculated by the Monte Carlo method. From the collision probability results of 500 Gaussian mixture components and 5000 Gaussian mixture components, the number of Gaussian mixture components clearly affects the collision probability accuracy. Ultimately, in the covariance propagation process, the accuracy of the collision probability calculation in the non-Gaussian case can be effectively improved by increasing the number of Gaussian mixture components.

4. Conclusions

The propagation of a space object's orbital state and uncertainty is a nonlinear dynamic process, and the propagation of orbit error will following a non-Gaussian distribution assuming that the initial orbital uncertainty is large or the forecast period is long. In the propagation with a linear method, the first partial derivative is obtained by series expansion while ignoring the influences of higher-order terms. The UKF method approximates the orbital uncertainty distribution by taking symmetric 2n+1 sampling points of the n-dimensional orbital state. An analysis of the simulation results of two scenarios reveals that the linear method and UKF method can be used as the simplest methods to propagate the orbital uncertainty and calculate the collision probability with a small initial orbital uncertainty. However, if the initial uncertainty is large, the orbital error distribution will not retain a Gaussian distribution. Fortunately, this non-Gaussian character can be captured by the Gaussian mixture method, and thus, the Gaussian mixture method is able to calculate the collision probability under the condition of non-Gaussian uncertainty propagation.

The Gaussian mixture method proposed in this paper is a weighted sub-Gaussian mixture algorithm based on a particle filter algorithm. Compared with the univariate splitting method, the advantage of this Gaussian mixture method is that it does not need to search for the most nonlinear direction. The orbital uncertainty accuracy represented by this Gaussian mixture method is correlated with the number of Gaussian mixture components: the more Gaussian mixture components there are, the higher the accuracy of the uncertainty representation will be. From the calculation results of the two simulation scenarios, this Gaussian mixture algorithm can effectively fit the uncertainty distribution of the orbital error regardless of whether the orbital uncertainty follows a Gaussian distribution or a non-Gaussian distribution. Moreover, the collision probability calculated by the Gaussian mixture algorithm is as accurate as that calculated by the Monte Carlo method. An analysis of the results of the two simulated scenario demonstrates that the number of sub-Gaussian mixtures is the key factor influencing the approximated distribution of the orbital uncertainty in the Gaussian mixture algorithm proposed in this paper. Therefore, increasing the number of sub-Gaussian mixtures can effectively improve both the fitting accuracy of the uncertainty distribution and the calculation accuracy of the corresponding collision probability.